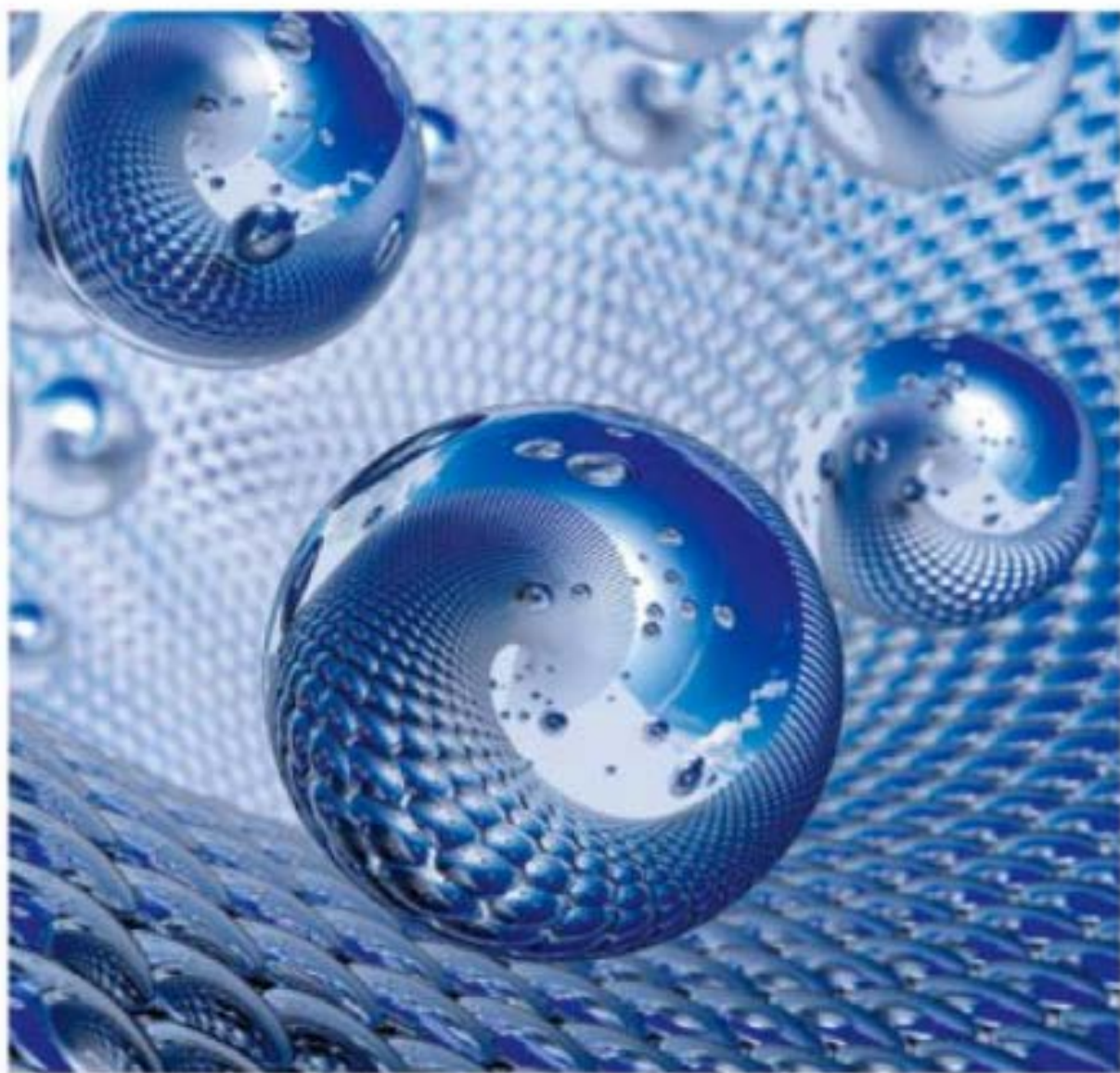


Edited by Joshua Edel and Tim Albrecht

# Nanopores for Bioanalytical Applications

Proceedings of the International Conference



RSC Publishing

1 SINGLE-MOLECULE DNA TRANSLOCATION THROUGH  $\text{Si}_3\text{N}_4$ - AND GRAPHENE  
2 SOLID-STATE NANOPORES  
3  
4  
5  
6  
7

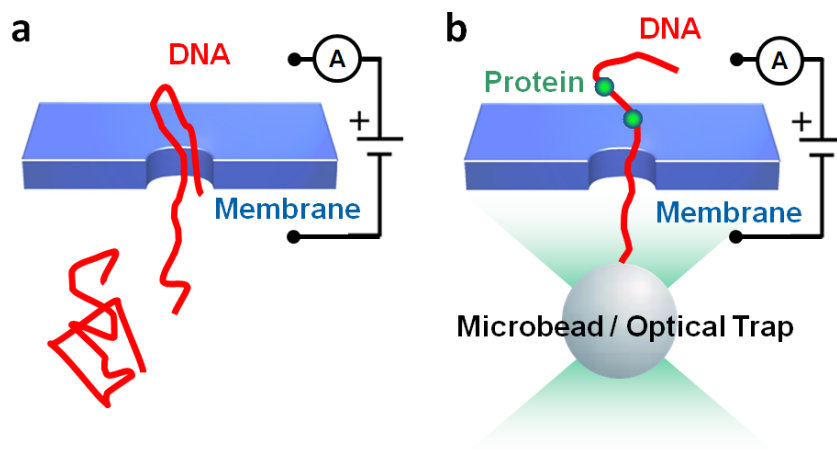
8 A. Spiering<sup>1</sup>, S. Knust<sup>1</sup>, S. Getfert<sup>1</sup>, A. Beyer<sup>1</sup>, K. Rott<sup>1</sup>, L. Redondo<sup>2</sup>, K. Tönsing<sup>1</sup>, P.  
9 Reimann<sup>1</sup>, A. Sischka<sup>1</sup> and D. Anselmetti<sup>1</sup>

10  
11 <sup>1</sup>Faculty of Physics, Bielefeld University, D-33615 Bielefeld, Germany

12 <sup>2</sup>Institut de Bioenginyeria de Catalunya (IBEC), University of Barcelona, Department of  
13 Chemical Physics, Faculty of Chemistry, 08028 Barcelona, Spain  
14  
15

16 1 INTRODUCTION  
17

18 The controlled translocation of a single, double-stranded DNA (dsDNA) through a solid-  
19 state nanopore (NP)<sup>1,2</sup> with optical tweezers (OT) is described in the presence of an electric  
20 field under buffer conditions. Upon threading dsDNA complexed by single proteins  
21 through a NP in 20 nm thick  $\text{Si}_3\text{N}_4$ -membranes, we find distinct asymmetric and retarded  
22 force signals that critically depend on the overall charge of the protein, the molecular  
23 elasticity of the dsDNA and the counter-ionic shielding of the polyelectrolyte (dsDNA) in  
24 the buffer<sup>3</sup>. This force response can be quantitatively simulated and understood within a  
25 theoretical model where an isolated charge on an elastic, polyelectrolyte strand experiences  
26 a harmonic nanopore potential during translocation. In order to extend these experiments to  
27 atomically thin solid-state NP, dsDNA was threaded through single nanolayer graphene  
28 NP by a transmembrane voltage. Whereas distinct single-molecule threading signals could  
29 here be observed in a Coulter counter setup (Fig. 1a) and compare well with recent  
30 papers<sup>4,5</sup>, OT controlled dsDNA-translocation through graphene NPs remained  
31 challenging, however (Fig. 1b). In this paper, we will give a current status report on optical  
32 tweezers controlled translocation through solid-state NPs.  
33



34  
35  
36 **Figure 1** (a) Coulter counter set-up for single-molecule NP translocation and ionic  
37 current detection. (b) Optical tweezers setup for measuring and controlling dsDNA NP  
38 translocation.  
39

## 2 METHOD AND RESULTS

### 2.1 Optical Tweezers Setup and Experimental Procedure

We used a single-beam, 3D quantitative OT system with confocal light guiding that incorporates an optical obstruction filter eliminating all axial light components and allowed manipulation and interference-free steering of polystyrene (PS) microbeads under buffer conditions in the vicinity of a reflecting interface (membrane)<sup>6</sup>. Individual Lambda ( $\lambda$ ) bacteriophage dsDNA molecules (48502 basepairs (bp), 16.4  $\mu\text{m}$  contour length) were functionalized at one end with several biotins and individually attached to a streptavidin-coated PS bead (3,28  $\mu\text{m}$  diameter). The dsDNA-bead constructs were kept in buffer solution (20 mM / 1M KCl and 2 mM Tris/HCl at pH 8.0) at 22°C and introduced into our NP fluidic cell prior conducting the experiment. In order to probe the force response of an individual protein attached to dsDNA when being threaded through a NP, we introduced either EcoRI (31 kDa) or RecA (38 kDa) proteins.

### 2.2 Nanopore Fabrication

Solid-state NPs in 20 nm thick  $\text{Si}_3\text{N}_4$ - and single nanolayer graphene membranes were produced by helium-ion microscope milling (Orion, Zeiss, Oberkochen), rendering NP openings with diameters typically 20-60 nm in size.

### 2.3 Graphene Preparation and Electrical Characterization

Single and multiple graphene nanolayers have been mechanically exfoliated and transferred onto a 20 nm thick  $\text{Si}_3\text{N}_4$ -membrane via the “wedging transfer” technique<sup>5,7</sup> over a 5  $\mu\text{m}$  wide hole that was etched into the  $\text{Si}_3\text{N}_4$ -membrane. Since special emphasis has been put on virtually void-free graphene nanolayers for high electrical transmembrane resistance, we used pristine, naturally grown single-crystal graphite nanoflakes (NGS Naturgraphit, Leinburg). In Fig. 2a, a graphene sample with one to three nanolayers is shown in a light microscopy image. A representative current-voltage (I-V) characteristics of a single nanolayer graphene is shown in Fig. 2b, exhibiting an electrical resistance of 29 G $\Omega$  in 20 mM KCl buffer solution (Gigaohm seal) as it could only be found in the measured pristine graphene flakes. A 20 nm wide, single nanolayer graphene NP is shown in Fig. 2c. The extraordinary image

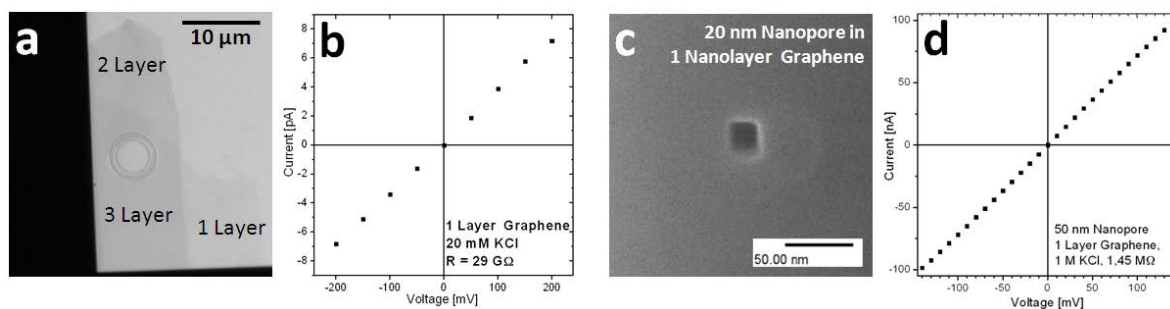


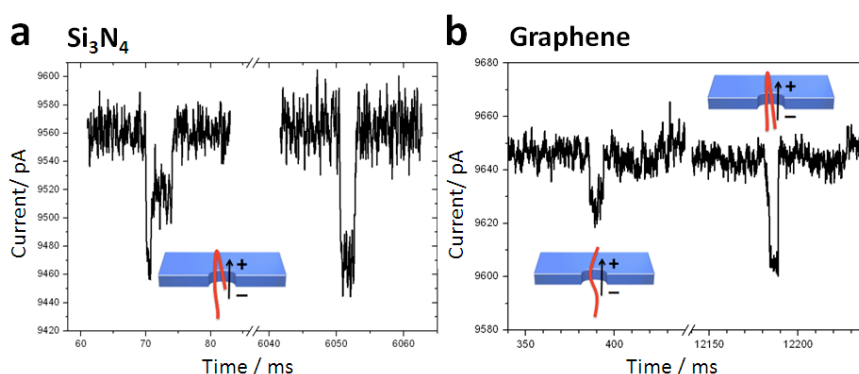
**Figure 2** (a) One to three nanolayer graphene sample transferred to  $\text{Si}_3\text{N}_4$ -membrane. (b) I-V curve of single nanolayer graphene with Gigaohm seal. (c) 20 nm wide NP fabricated in graphene nanolayer by He-ion microscopy milling. (d) 1,45 M $\Omega$  contact resistance of 50 nm single nanolayer graphene NP recorded in 1M KCl.

1 contrast is due to the He-ion microscope technology that has also been used to drill the NP.  
2 In Fig. 2d, an I-V-curve of an 50 nm wide graphene NP is shown, exhibiting an NP  
3 resistance of 1,45 M $\Omega$  recorded in 1M KCl. In that respect two aspects are worth noting: 1)  
4 although control experiments always indicated proper NP fabrication, rather frequently we  
5 failed to measure a distinct NP electrical contact resistance even when occasionally  
6 surfactants were added to the solution to improve surface wetting, and 2) the measured NP  
7 resistance complies well with other data<sup>5</sup> extrapolated for a 50 nm NP.

### 8 9 3 RESULTS AND DISCUSSION

#### 10 11 3.1 dsDNA Coulter Counter Experiments

12  
13 After adding linear  $\lambda$ -DNA to the cis-compartment of our microfluidic cell device<sup>6</sup>, and  
14 applying an electrical transmembrane voltage (trans: positive, cis: negative) reproducible  
15 single-molecule DNA translocation events could be discerned for both Si<sub>3</sub>N<sub>4</sub>- as well as  
16 single nanolayer graphene NPs. In Fig. 3a and b, representative translocation signals are  
17 given, reflecting the expected ionic-current blockade during dsDNA translocation for 1 M  
18 KCl buffer solution. As already indicated in previous publications, the current variations  
19 reflect the folding configuration of the translocating dsDNA-molecules<sup>4,5,8</sup>.



21  
22  
23 **Figure 3** (a) Coulter counter signals of two  $\lambda$ -DNA single-molecule NP translocation  
24 events through a Si<sub>3</sub>N<sub>4</sub>-NP with a diameter of 40 nm (transmembrane voltage 40 mV). (b)  
25 Corresponding signals of  $\lambda$ -DNA single-molecule NP translocation events through a single  
26 nanolayer graphene NP with a diameter of 20 nm (transmembrane voltage 140 mV). The  
27 current variations are due to the ionic-current blockade and reflect the folding  
28 configuration of the translocating DNA.

#### 29 30 3.2 Translocation of Protein-complexed dsDNA with Optical Tweezers (Si<sub>3</sub>N<sub>4</sub>-NP)

31  
32 Since we are interested in the quantification of the associated physical mechanisms during  
33 molecular translocation, we attached the dsDNA-molecule to a PS-microbead that could be  
34 trapped, steered and monitored with our OT setup (Fig. 1b). Upon approaching the NP  
35 with a DNA-functionalized microbead and applying a transmembrane voltage (trans:  
36 positive) the DNA gets threaded into the NP which can be monitored as a constant force  
37 signal. A representative example is depicted in Fig. 4a, where the dsDNA is actively being  
38 pulled out of the NP by moving back the microbead with the OT. The jump from the 11 pN  
39 background force to zero reflects the threading out of the DNA from the NP. In addition,  
40 two characteristic asymmetric force fingerprints (dips) with a retarded force increase  
41 extending over more than 200 nm, can be discerned. Each of these asymmetric

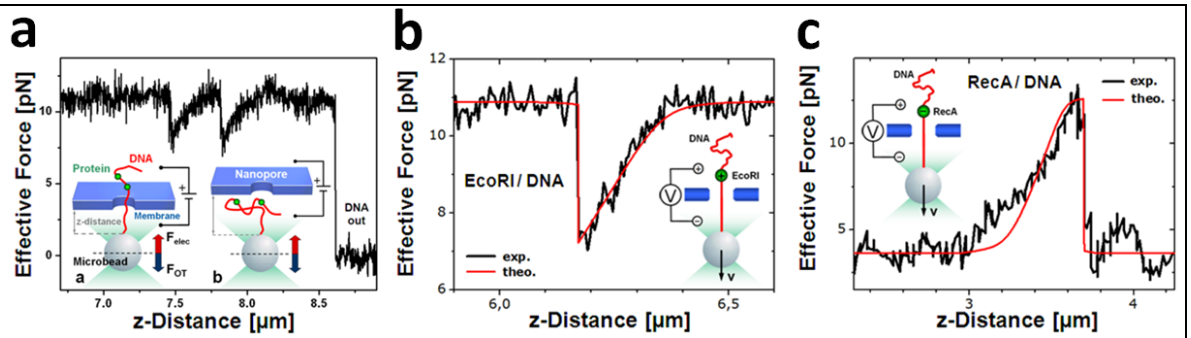


**Figure 4** (a) Force response signal of a protein-complexed  $\lambda$ -DNA-molecule that is being threaded out of a  $\text{Si}_3\text{N}_4$ -NP by OT (45 nm NP diam., 50mV). (b) Close-up of a single-molecule EcoRI/DNA-complex force fingerprint (dip) during NP translocation (45 nm NP diam., 50mV). (c) Force response (peak) of a RecA-complexed  $\lambda$ -DNA-molecule (45 nm NP diam., 20mV). The experimental force response curves (black) in b) and c) were theoretically simulated according a stochastic model<sup>3</sup> (red), yielding the effective protein charge as a result ((b)+59,5e for EcoRI; (c) -700e for RecA-Oligomer ) (Figures adapted from Ref. 3).

force signals can be attributed to a single EcoRI-protein that is translocating through the  $\text{Si}_3\text{N}_4$ -NP (Fig 4b). As we could show in an earlier paper<sup>3</sup>, this single protein force signal depends on the effective protein charge. Hence and in contrast to the positively charged EcoRI protein, the force response of negatively charged RecA-proteins leads to an inverted force signal (peak), as it is shown in Fig. 4c.

The experimental force curves could quantitatively be simulated within a theoretical model where an isolated charge on an elastic, polyelectrolyte strand experiences a harmonic nanopore potential during translocation<sup>3</sup>. As a consequence one finds that the total NP potential for a translocating protein (under external mechanical control) exhibits two minima (potential wells) with a barrier (saddle) in between, corresponding to two metastable “states” with the charged protein on either side of the membrane. As the OT moves, the protein translocates through the NP, however, not in a uniform way but with a dynamics that is governed by thermal fluctuations inducing stochastic transitions between

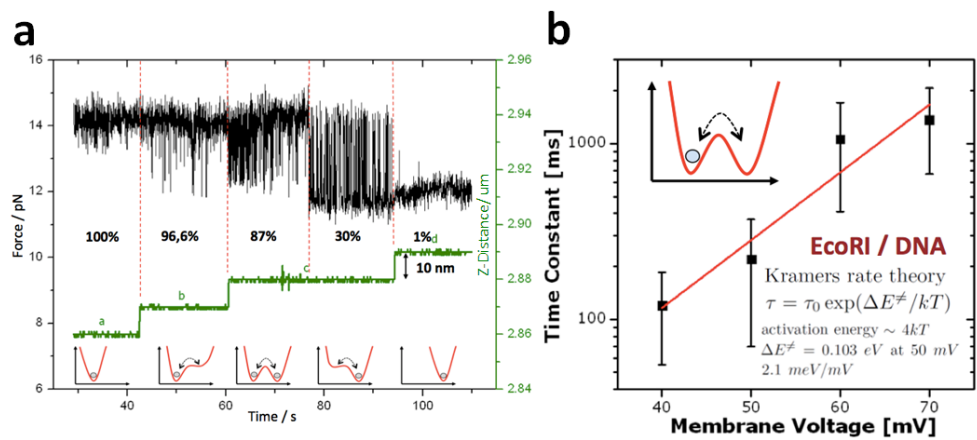


**Figure 5** (a) Thermally activated stochastic transition between the two NP states as can be discerned from the experimental force response curve. The balance between the two-state system can be controlled by the position of the protein along the NP axis coordinate. (b) Estimate of the activation energy between the two NP-states yielding  $\sim 4kT$  at a transmembrane voltage of 50 mV.

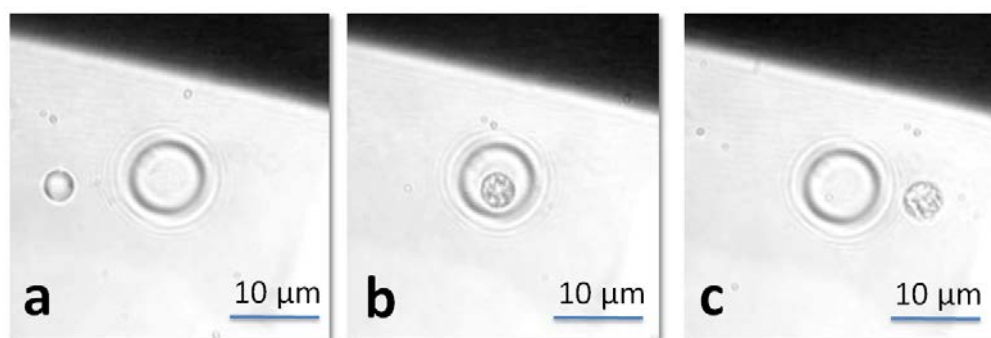
1  
2  
3  
4  
5  
6  
7  
8  
9  
10  
11  
12  
13  
14  
15  
16  
17  
18  
19  
20  
21  
22  
23  
24  
25  
26  
27  
28  
29  
30  
31

1 the two states (Fig. 5a). Since these transitions depend on the applied membrane voltage  
2 (via the effective NP potential), the measured (averaged) fluctuation time can be related to  
3 the activation energy between the two NP states (Kramers rate theory) (see also Fig. 5b).

### 4 5 **3.3 Towards Translocation of dsDNA with Optical Tweezers (Graphene-NP)**

6  
7 Since the above physical translocation mechanism is governed by non-equilibrium  
8 dynamics and depends on the experimental boundary conditions like protein net charge,  
9 transmembrane voltage, NP diameter, membrane thickness, ionic buffer strength,  
10 electroosmotic currents through the NP (via NP surface charge) and others, it would be  
11 insightful to investigate this phenomenon in more detail with other NP geometries and  
12 materials. Therefore we chose graphene for this purpose and prepared single nanolayer  
13 graphene which we transferred onto  $\text{Si}_3\text{N}_4$ -membrane supports. The milled graphene NPs  
14 with typical diameters of 20-50 nm were tested in Coulter counter experiments (see Figs. 2  
15 and 3), where we monitored individual DNA-passages through the NP.

16 In contrast, OT-controlled translocation experiments as described in chapter 3.2 for  $\text{Si}_3\text{N}_4$ -  
17 NP turned out to be challenging for graphene NP. The reason might be a systematic  
18 difficulty, which stems from the fact that a PS-microbead – optically trapped in a strong  
19 IR-laser focus - is obviously heavily thermally activated in the presence of a graphene  
20 interface (Fig. 6). This observation suggests that at least the glass transition temperature of  
21 PS (around 100 °C) is reached, however, no other phenomena (strong convective flow or  
22 vapor microbubbles) can additionally be found. Nevertheless, if this assumption would  
23 hold, the integrity of PS-microbead, the dsDNA and its biotin-avidin fixation to the  
24 microbead would be questionable<sup>9,10</sup>.



26  
27  
28 **Figure 6** (a) Video series of light microscopy images, where a PS-microbead (3,28  $\mu\text{m}$   
29 diam.) is positioned with a focussed IR-laser (OT) a few micrometers away from a  $\text{Si}_3\text{N}_4$ -  
30 membrane where a single nanolayer graphene is transferred to. The round bore in the  
31 middle of the image is a micropore ( $\sim 10 \mu\text{m}$  diam.) in the  $\text{Si}_3\text{N}_4$ -membrane window and  
32 hosts a free-standing graphene nanolayer (Almost the complete  $\text{Si}_3\text{N}_4$ -membrane is also  
33 coated by the graphene). Upon laterally moving the microbead in constant distance across  
34 the micropore (with constant laser trapping power of 200 mW), the microbead gets almost  
35 instantaneously "heated" only when positioned over the free-standing graphene and turns  
36 opaque.

#### 37 38 **4 CONCLUSION**

39  
40 The translocation of linear (protein-complexed)  $\lambda$ -DNA through  $\text{Si}_3\text{N}_4$ - and single  
41 nanolayer graphene nanopores was investigated with a Coulter counter based setup as well

1 as with optical tweezers control. For the OT controlled translocation experiments through  
2 solid-state Si<sub>3</sub>N<sub>4</sub>-NP, our results provide convincing evidence that force-controlled  
3 translocation dynamics of a polyelectrolyte through a NP is accompanied by a  
4 thermally induced, stochastic hopping between two adjacent NP states that can  
5 adequately be described by Kramers rate theory. Beyond the possibility to detect and  
6 reversibly control the position of a single translocating protein attached to a DNA  
7 strand by OT, obviously, the overall elasticity of the DNA-polymer significantly  
8 contributes to the retarded force response signals when threaded through a NP. It  
9 will be interesting to see how force controlled detection concepts will contribute to  
10 single molecule NP-based spectroscopy and analysis in the future.

## 11 ACKNOWLEDGEMENTS

12 We would like to thank Dieter Akemeier, Christoph Pelargus, Helene Schellenberg for  
13 technical assistance as well as many stimulating discussions with Cees Dekker, Ulrich  
14 Keyser, Armin Götzhäuser and Andreas Hütten. Financial support from the Collaborative  
15 Research Centre 613 of the Deutsche Forschungsgemeinschaft (DFG) is gratefully  
16 acknowledged.  
17  
18  
19  
20

## 21 References

- 22 1 U. F. Keyser, B. N. Koeleman, S. van Dorp, D. Krapf, R. M. M. Smeets, S. G. Lemay, N. H.  
23 Dekker and C. Dekker, *Nature Physics*, 2006, **2**, 473.
- 24 2 A. Sischka, A. Spiering, M. Khaksar, M. Laxa, J. König, K.-J. Dietz, and D. Anselmetti, *J. Phys:*  
25 *Condens. Matter*, 2010, **22**, 454121.
- 26 3 A. Spiering, S. Getfert, A. Sischka, P. Reimann, and D. Anselmetti, *NANO Letters*, 2011, **11**,  
27 2978.
- 28 4 C. A. Merchant, K. Healy, M. Wanunu, V. Ray, N. Peterman, J. Bartel, M. D. Fischbein, K.  
29 Venta, Z. Luo, A. T. C. Johnson, M. Drndic, *NANO Letters*, 2010, **10**, 2915.
- 30 5 G. F. Schneider, S. W. Kowalczyk, V. E. Calado, G. Pandraud, H. W. Zandbergen, L. M. K.  
31 Vandersypen and C. Dekker, *NANO Letters*, 2010, **10**, 3163.
- 32 6 A. Sischka, Ch. Kleimann, W. Hachmann, M. M. Schäfer, I. Seuffert, K. Tönsing, and D.  
33 Anselmetti, *Rev. Sci. Instrum.* 2008, **79**, 063702.
- 34 7 G. F. Schneider, V. E. Calado, H. Zandbergen, L. M. K. Vandersypen, and C. Dekker, *NANO*  
35 *Letters*, 2010, **10**, 1912.
- 36 8 R. M. M. Smeets, U. F. Keyser, D. Krapf, M.-Y. Wu, N. H. Dekker, and C. Dekker, *NANO*  
37 *Letters*, 2006, **6**, 89.
- 38 9 M. González, C.E. Argaraña, G. D. Fidelio, *Biomol. Eng.*, 1999, **16**, 67.
- 39 10 Y. Li, Y. Fan, J. Ma, *Polym. Degrad. Stab.* 1999, **65**, 395.
- 40  
41  
42